Research Square

Preprints are preliminary reports that have not undergone peer review.
They should not be considered conclusive, used to inform clinical practice,
or referenced by the media as validated information.

Structural, Thermal, Morphological, and Shape Memory Properties of Silicone-Reinforced PVA/PEG Composite Films

Gülistan AKKAYA SELÇİN

gakkaya@beu.edu.tr

Bitlis Eren University

Meltem COŞKUN

Firat University

Ercan ERCAN

Bitlis Eren University

Research Article

Keywords: Polyvinyl alcohol (PVA), Polyethylene glycol (PEG), Silicone composites, Thermal stability, Flexible materials

Posted Date: August 13th, 2026

DOI: https://doi.org/10.21203/rs.3.rs-9912868/v1

License: This work is licensed under a Creative Commons Attribution 4.0 International License.
Read Full License

Additional Declarations: No competing interests reported.

Abstract

Absract

In this study, silicone-reinforced PVA/PEG composite films were successfully prepared using the solution casting method. Polyvinyl alcohol (PVA) was used as the polymer matrix, polyethylene glycol (PEG) as the plasticizer, and silicone as the reinforcing phase. Silicone was incorporated into the polymer blend at different weight ratios (5%, 10%, 20%, and 30%) in order to investigate its influence on the structural, thermal, and morphological properties of the composites. The prepared films were characterized using X-ray diffraction (XRD), Fourier transform infrared spectroscopy (FTIR), thermogravimetric analysis (TGA), differential scanning calorimetry (DSC), and scanning electron microscopy (SEM). XRD results revealed that increasing silicone content promoted structural ordering and enhanced the crystallinity of the composites. FTIR spectra confirmed the presence of intermolecular interactions between the polymer matrix and silicone phase without the formation of new chemical bonds. TGA analysis demonstrated that silicone incorporation improved the thermal stability and increased the residual mass at elevated temperatures due to the thermally stable Si–O–Si structure. DSC findings indicated that silicone affected both the amorphous and crystalline regions of the polymer matrix, leading to modifications in glass transition and melting behavior. SEM observations showed a relatively homogeneous dispersion of silicone within the PVA/PEG matrix, particularly at moderate filler concentrations. Overall, the results suggest that silicone-reinforced PVA/PEG composites exhibit improved structural and thermal properties, making them promising candidates for flexible, lightweight, and multifunctional material applications.

1. Introduction

Among various polymers, polyvinyl alcohol (PVA), a biodegradable and synthetic polymer, stands out as a promising matrix material owing to its excellent film-forming ability, high dielectric strength, high tensile strength, non-toxicity, and biocompatibility [1–2]. Due to these unique properties, PVA has been used in pharmaceutical industries, electronics, optical sensors, food packaging, and biomedical applications [3–5]. Despite these advantages, neat PVA films often suffer from limited mechanical strength and thermal stability, which restricts their application in areas requiring durability and elastomeric behavior [6]. To overcome these shortcomings, researchers frequently employ strategies such as polymer blending and the addition of plasticizers or nanofillers [7–9]. Polyethylene glycol (PEG) is a synthetic, hydrophilic polymer synthesized through the anionic polymerization of ethylene oxide monomers, renowned for its biocompatibility and non-toxic profile [10–12]. It is widely recognized as a highly efficient phase change material (PCM) for latent heat thermal energy storage due to its high energy storage density, appropriate phase change temperature ranges, and favorable thermal stability [13–15]. Polyethylene glycol (PEG) is a widely used plasticizer because of the strong hydrogen bonds that form between the hydroxyl groups of the PVA backbone and the ether bonds in the PEG chains[16]. The inclusion of PEG increases the free volume within the polymer matrix, thereby enhancing the flexibility, ductility, and processability of the resulting blend [17]. To further optimize the physical

properties of these blends, inorganic fillers are incorporated into the polymer matrix [18–20]. A key factor governing the final properties of composite materials is the filler loading ratio. The concentration of the dispersed phase directly influences the homogeneity of the mixture, the percolation threshold and the nature of the polymer-filler interface, ultimately dictating the mechanical performance and structural integrity of the composite. Systematic investigation of these effects is therefore essential.

Silicone presents a compelling candidate as a filler, is known to improve surface characteristics, thermal stability, and mechanical toughness when introduced into polymeric systems [21]. By dispersing silicone within a PVA/PEG matrix, it is planned to create a hybrid composite that synergizes the strength and hydrophilicity of PVA with the flexibility imparted by PEG and the unique characteristics of silicone. Thus, these types of materials can be used in potential applications such as specialized coatings, flexible packaging, biomedical devices, or soft electronics where a balance of strength, flexibility, and environmental resistance is required. Theoretical studies in the literature show that the PVA-PEG-Si structure exhibits good thermal properties and, due to its low cost, offers significant potential for lightweight applications in photonics and optoelectronics[22].

Numerous investigations have explored the enhanced characteristics of PVA/PEG matrix systems in the literature [19, 20]. The incorporation of metal oxide nanoparticles into the PVA/PEG matrix effectively tailors the electrical, optical and mechanical properties of the resulting nanocomposites. Due to its unique properties, MgO is a highly suitable metal oxide for use in research. The addition of MgO nanoparticles within the PVA/PEG polymer matrix improved the material's hydrophilicity, mechanical strength, and thermal stability, which promotes better cell adhesion and faster healing[23]. Likewise, incorporation of AZO nanoparticles enhances the films' electrical conductivity and hydrophobicity while reducing the optical band gap. Furthermore, the resulting films demonstrate significant antibacterial activity against various pathogenic bacteria, which improves as the filler concentration increases. These findings suggest that the prepared multifunctional films are strong candidates for applications in optoelectronic devices, food packaging, and biomedical fields [24]. Increasing the concentration of metal oxide nanoparticles, such as In_2O_3, $BaTiO_3$, $Cr2O_3$ in PVA/PEG mixtures leads to a significant increase in dielectric constant, dielectric loss, and AC conductivity, making these mixtures suitable for various electronic nano devices. Additionally, it significantly increases optical absorption and reduces the energy band gap, making them suitable for optoelectronic applications [25–27]. Similarly, incorporating nano Gd_2O_3 into a PVA/PEG matrix increases structural disorder and affects thermal stability, specifically increasing the melting temperature while reducing the degradation temperature [28]. On the other hand, the incorporation of SiO_2/CuO hybrid nanoparticles into the PVA–PEG matrix significantly enhances the material's optical and dielectric properties. Also, PVA–PEG–SiO_2/CuO nanostructures exhibit high sensitivity and environmental resistance, making them ideal candidates for flexible pressure sensors [29]. In another study, increasing the concentration of SiO_2-$Co2O_3$ hybrid nanoparticles in the PVA–PEG matrix significantly enhanced optical parameters, including absorbance and refractive index, while reducing the energy gap. Thus, the potential in the field for optoelectronics applications has been demonstrated [30]. TiN has been sought for the past thirty years owing to its unique properties. PVA/

PEG nanocomposites doped with increasing concentrations of TiN NPs enhance the material's absorbance, refractive index, and optical conductivity, while simultaneously decreasing the transmittance and the optical energy gap for both allowed and forbidden indirect transitions. Based on these improved optical characteristics, the research concludes that PVA/PEG/TiN nanocomposites are suitable candidates for optoelectronic detector applications. In another study, the results indicated that increasing the TiN-nanoparticles' concentration leads to improved A.C. electrical conductivity, suggesting a high potential for use in nanoelectronic applications [31, 32].

As seen, while much of the current literature focuses on metal oxide nanoparticles as fillers for PVA/PEG systems, the synergistic effect of varying concentrations of silicone as a primary reinforcement phase in a solution-casted PVA/PEG matrix remains an area requiring further investigation. Furthermore, although silicone-modified hydrogel sensors have been investigated, the systematic characterization of silicone-filled PVA/PEG composite films obtained by solution casting, which balances the high ductility provided by liquid PEG with the structural integrity of silicone, has not been fully addressed in the literature. In this study, we report the preparation and characterization of a series of novel composite films based on a PVA matrix plasticized with liquid PEG and reinforced with varying weight percentages of silicone. The aim is to understand the impact of silicone incorporation on the structural, morphological, and physical properties of the PVA-PEG-based nanocomposite films.

2. Materials and Methods

2.1. Preparation of Composite Samples

In this study, polyvinyl alcohol (PVA) was used as the matrix phase, liquid polyethylene glycol (PEG) as the plasticizer, and silicone as the filler phase. Pure water was chosen as the solvent medium. First, pure water was heated to a temperature range of 85–90°C. 0.4 g of PVA was added to the heated pure water. To ensure complete dissolution of the PVA, the solution was stirred for approximately 1 hour using a magnetic stirrer and magnetic bar. At the end of this period, a homogeneous PVA solution was obtained. After the PVA dissolved, 0.1 gr of liquid PEG were added to the solution as a plasticizer, and the mixing process was continued for approximately 15 more minutes. This created a PVA/PEG-based polymer matrix. The resulting mixture was blended to increase its homogeneity. Composites containing different proportions of silicone were produced using the prepared base mixture. Silicone was added to the mixture at proportions of 5%, 10%, 20%, and 30% by weight. The same experimental procedure was applied for each silicone proportion. After the addition of silicone, the mixtures were immersed in a magnetic stirrer with a mixer tip and stirred at high speed for approximately 1 hour and 25 minutes. At this stage, the silicone was homogenously dispersed within the polymer matrix. The experimental conditions were kept constant throughout the mixing period. The prepared composite solutions were poured into Petri dishes and dried in an oven for 24 hours to completely remove the solvent. As a result, PVA/PEG-based silicone-reinforced composite materials with different silicone ratios were prepared. The obtained samples were used in characterization and performance tests carried out in subsequent stages.

2.2. Characterizations

Characterization encompasses analyses conducted to determine the physical, chemical, thermal, and structural properties of a material. In this study, Fourier transform infrared spectroscopy (FTIR), X-ray diffraction (XRD), thermogravimetric analysis (TGA), differential scanning calorimetry (DSC), and scanning electron microscopy (SEM) analyses were used. FTIR analysis was performed in the 3500–500 cm^{-1} range to identify functional groups and chemical bonds in the material. XRD analysis was performed in the 10–80° 2θ range to investigate crystalline phases and crystallinity behavior. TGA measurements were conducted in the approximate 25–500°C temperature range to evaluate the thermal decomposition behavior of the samples. DSC analyses were performed in the 25–200°C range to determine the glass transition, melting, and crystallization temperatures. SEM analysis was conducted at different magnifications to examine the surface morphology and filler distribution of the samples.

3. Results and Discussion

3.1. Crystal structure

Upon examination of the X-ray diffraction (XRD) patterns shown in Fig. 1, it is observed that the pure “Blend” sample exhibits a broad diffraction band in the range of approximately 2θ ≈ 20–25°[33, 34]. This indicates that the material has a largely amorphous structure[35, 36]. With the addition of the additive (G1: 5%, G2: 10%, G3: 20%, and G4: 30%), distinct changes are observed in the XRD patterns. In particular, the high-intensity and sharper peaks appearing in the 20–30° and 40–60° (2θ) ranges indicate an increase in the degree of crystallinity in the system[37, 38]. This is more pronounced in the G3 and G4 samples, suggesting the formation of ordered crystalline regions within the structure[39, 40]. Furthermore, the decrease in peak widths (FWHM narrowing)[41], as the filler content increases indicates that the crystallite size is growing. This behavior is attributed to the filler particles acting as heterogeneous nucleation sites within the matrix. These centers promote crystal growth by facilitating a more ordered arrangement of polymer chains[42, 43]. In the G1 (5%) and G2 (10%) samples with low filler content, the coexistence of a broad amorphous band and weak crystalline peaks indicates that these systems are in a semi-crystalline transition region. This indicates that crystallization begins at low filler concentrations but becomes dominant at higher concentrations[44, 45]. Consequently, it is clearly observed that as the filler content increases, the material’s structural order increases, and the system transitions from an amorphous structure to a semi-crystalline and subsequently a distinct crystalline structure. These results are consistent with similar studies in the literature[46–49].

3.2.FTIR (Fourier Transform Infrared Spectroscopy)

The FTIR analyses shown in Fig. 2 were conducted to comparatively evaluate the chemical structure and interphase interactions of PVA/PEG composites containing different proportions of silicon. Upon examination of the obtained spectra, the broad band observed in the 3200–3500 cm^{-1} range in all samples corresponds to –OH stretching vibrations associated with hydrogen bonds and originates from

the hydroxyl groups in the PVA and PEG structures[50]. Although no significant shift in position was observed in this band with increasing silicon content, slight increases in band width occurred, indicating that hydrogen-bond interactions have partially strengthened[51, 52]. It was observed that the bands corresponding to C–H stretching vibrations in the 2900–2940 cm^{-1} range had similar intensities in all samples and were not significantly affected by the addition of silicon. The H–O –H bending vibration peak, identified around 1650 cm^{-1}, was present in all composites and did not show a noticeable change depending on the silicon content[52]. In contrast, significant changes were observed in the bands in the 1000–1100 cm^{-1} range, depending on the silicon content. While C–O stretching vibrations were dominant in this region in the pure PVA/PEG sample, it was found that as the silicon content increased, the bands corresponding to Si–O–Si asymmetric stretching vibrations became more pronounced and the peak intensity increased. In particular, the fact that this band becomes sharper and more intense in samples with high silicon content indicates that the silicon phase is present in increasing amounts within the matrix and is successfully dispersed[53]. Similarly, it was observed that the bands corresponding to Si–O and Si–C vibrations in the 800–850 cm^{-1} range were weak at low silicon concentrations but became distinct as the silicon content increased. This confirms the presence of the silicon phase within the composite structure and the strengthening of its structural effect with increasing addition ratio[54]. The increase in silicon content did not lead to the formation of new chemical bonds in the FTIR spectra but caused changes in the intensity of existing peaks. This indicates that physical interactions, rather than chemical reactions, dominate in the composite system and that the silicon phase disperses within the polymer matrix without altering the chemical structure[55, 56]. The identified FTIR absorption bands are summarized in Table 1.

Table.1. FTIR spectra of PVA/PEG and silicon-filled composites

Wavenumber (cm^{-1})	Functional Group	Vibration Type	Observed in Samples
3200–3500	–OH	Stretching	All samples
2900–2940	C–H	Stretching	All samples
~ 1650	H–O–H	Bending	All samples
1080–1140	C–O	Stretching	Blend & composites
1000–1100	Si–O–Si	Asym. Stretch	Silicone samples
800–850	Si–C / Si–O	Bending	Silicone samples

3.3. Thermogravimetric Analysis (TGA)

The thermal degradation behavior of PVA/liquid PEG-based composites containing silicone additives at different concentrations (5–10% and 20–30%) was investigated via TGA analysis (Fig. 3). A multi-step degradation profile was observed in all samples. The low-level mass loss below 150°C is attributed to the release of physically adsorbed moisture resulting from PVA's hydrophilic nature. It has been extensively reported in the literature that the hydroxyl groups in PVA chains form hydrogen bonds with

water, leading to moisture loss at low temperatures[57]. The hygroscopic nature of PEG may also contribute to this initial mass loss. The main degradation stage occurred in the temperature range of approximately 250–350°C. In this region, when PVA is heated, it first loses water to form conjugated structures containing consecutive double bonds. Subsequently, these structures become unstable, and the polymer's main chain breaks. It has been comprehensively demonstrated that the thermal degradation mechanism of PVA proceeds first through water elimination, followed by chain scission[58]. The plasticizing effect of PEG can cause a slight decrease in the onset temperature of degradation by increasing polymer chain mobility; this has been previously reported in PVA systems containing PEG[59]. It was observed that the decomposition rate decreases at temperatures above 350°C and that the formation of residue (char) becomes more pronounced. As seen in the graph, the amount of residue remaining in the high-temperature region increases as the silicon content rises. In particular, it is observed that the mass fraction remaining around 450°C is higher as the silicon content increases. This is explained by the high bond energy of the Si–O–Si bonds in the silicon structure and the formation of a silica-like thermally stable structure during degradation. For example, it has been extensively reported in the literature that silicone-based materials such as polydimethylsiloxane (PDMS) form an inorganic-enriched protective layer during thermal decomposition, which limits heat and mass transfer and thereby increases char yield[60].

3.4. DSC(Differential Scanning Calorimeter)

The effect of adding silicone at different ratios to PVA/PEG-based composites on their thermal behavior was investigated using differential scanning calorimetry (DSC) analysis. Upon examining the DSC curves presented in Fig. 4, the baseline shifts observed in the low-temperature region in all samples are considered to be related to moisture removal from the system and polymer chain mobility[61, 62]. The glass transition temperature (Tg), determined in the approximately 50–70°C temperature range, corresponds to the amorphous regions of the PVA and PEG phases. Partial changes in the Tg value were observed with an increase in the silicone content. This can be explained by the fact that silicone particles limit chain mobility by increasing interactions between polymer chains, causing the composite structure to acquire a stiffer character[63, 64]. The distinct endothermic peak observed in the DSC curves in the range of approximately 210–230°C is defined as the melting temperature (Tm) and primarily corresponds to the crystalline regions of PVA. As the silicon content increased, a decrease in the intensity and broadening of this peak occurred. This indicates that silicon partially inhibits the formation of crystalline structures, thereby reducing the system's degree of crystallinity [65]. However, the fact that a more stable thermal profile was obtained in samples with a high silicon content indicates that silicon acts as a filler material that enhances thermal stability within the composite structure. Consequently, it has been determined that the addition of silicon affects both the amorphous and crystalline phases and improves the overall thermal properties of the composite[65, 66].

3.5. SEM (Scanning Electron Microscope)

SEM images of the pure blend, 5% silicone and 30% silicone added blend composites are given in Fig. 5 .The SEM image of the pure blend sample shows that PVA's excellent film-forming ability and transparent structure enable the surface to exhibit a smooth and homogeneous appearance[12] The absence of large-scale phase separation confirms that PEG, acting as an effective plasticizer, has infiltrated between the PVA chains, enhancing chain mobility and preserving the amorphous structure. [67] This homogeneity originates from the strong intermolecular hydrogen bonds between the polymer components[34].With the addition of 5% silicone, characteristic changes begin to emerge in the surface morphology. The small-sized and dispersed particles observed within the matrix indicate that at this concentration, the silicone still exhibits a homogeneous distribution and achieves good interfacial

compatibility with the matrix.A silicone loading of 30% causes a dramatic transformation in the surface morphology. The large silicone agglomerates (clusters) prominent in the image demonstrate that at high filler concentrations, nanoparticles show an increased tendency to cluster among themselves[68]. This leads to a decline in the bonding quality at the matrix-filler interface, a reduction in elasticity, and the formation of macroscopic defects[69].The deep voids and cracks observed arise from the interfacial incompatibility that occurs when the filler content exceeds the critical threshold[70].This indicates that high additive ratios may compromise the structural stability of the material. As the silicone content increases, maintaining a homogeneous distribution within the PVA/PEG matrix becomes increasingly difficult and microstructural integrity deteriorates. At high loadings (particularly 30%), the thermodynamic incompatibility between silicone and PVA becomes pronounced, leading to interfacial defects that may adversely affect the mechanical properties. At low loadings (5%), the distribution quality remains at an acceptable level.

3.6. SME (Shape Memory Effect)

Figure 6 demonstrates the thermally induced shape memory behavior of the prepared composite film through successive deformation, fixation, and recovery stages. Initially, the sample exhibited its permanent flat configuration. Upon heating to approximately 75°C, the material became flexible and was easily deformed around a cylindrical rod, indicating that the polymer chains gained sufficient mobility above the transition temperature. After immersion in cold water, the temporary shape was successfully fixed, suggesting effective restriction of molecular motion through cooling-induced stabilization. When the deformed sample was subsequently exposed to hot water, it gradually recovered its original geometry, confirming the presence of a reversible shape memory effect[71].This behavior can be attributed to the thermomechanical response of polymeric shape memory systems, where temporary deformation is stabilized below the transition temperature and recovered upon reheating due to the elastic restoring force stored within the polymer network. The observed recovery mechanism is consistent with the classical shape memory cycle reported in the literature for thermally responsive polymer systems. The successful fixation and recovery behavior observed in the composite indicates that the material possesses good shape fixity and shape recovery capability. The incorporation of PEG and silicone likely contributed to enhanced chain flexibility and reversible molecular rearrangement during the heating–cooling cycle. PEG-containing polymer systems are known to facilitate reversible

switching behavior due to their flexible molecular chains and thermally responsive domains[72]. Furthermore, the nearly complete recovery of the original shape after reheating suggests that the composite structure can effectively store and release elastic deformation energy without significant permanent damage. Such behavior is highly desirable for applications including smart coatings, soft actuators, biomedical devices, flexible electronics, and thermally responsive materials. The results therefore demonstrate that the developed PVA/PEG-silicone composite exhibits promising potential as a thermally activated shape memory polymer system[73–75]

4. Conclusions

Silicone-filled PVA/PEG composite films were successfully fabricated via the solution casting technique, and the effects of different silicone concentrations on the material properties were systematically investigated. The characterization results demonstrated that silicone incorporation significantly influenced the structural, thermal, and morphological behavior of the composites. XRD analysis revealed that increasing silicone content enhanced the structural ordering and crystallinity of the composites by promoting heterogeneous nucleation within the polymer matrix. FTIR results confirmed the existence of physical interactions, mainly hydrogen bonding, between PVA, PEG, and silicone phases without altering the fundamental chemical structure of the system. Thermal analyses showed that silicone improved the thermal stability of the composites, particularly at high temperatures, due to the formation of thermally resistant Si–O–Si networks. DSC findings further indicated that silicone affected the thermal transitions of the polymer blend and contributed to a more stable composite structure. SEM images demonstrated that silicone was relatively well dispersed throughout the polymer matrix, although higher filler concentrations may lead to localized aggregation. The combination of PVA, PEG, and silicone resulted in composite films with enhanced thermal resistance, improved structural integrity, and favorable flexibility. The developed PVA/PEG-silicone composites exhibit considerable potential for advanced engineering and functional material applications such as flexible coatings, biomedical materials, soft electronic systems, packaging technologies, and lightweight multifunctional structures. Future studies may focus on mechanical, optical, dielectric, and biocompatibility investigations to further optimize the performance of these composite systems.

Declarations

Funding

The authors received no financial support for the research, authorship, and/or publication of this article.

Author Contribution

Author Contributions: Meltem Coşkun was responsible for conducting the experiments and preparing the figures. Gülistan Akkaya Selçin contributed to data analysis, interpretation of results, and literature

review. Ercan Ercan was responsible for image and graphical interpretation. All authors read and approved the final manuscript.

Data Availability

All data supporting the findings of this study are available within the paper and its Supplementary Information.

References

1. Aslam M, Kalyar MA, Raza ZA (2018) Polyvinyl alcohol: A review of research status and use of polyvinyl alcohol based nanocomposites. Polym Eng Sci 58(12):2119–2132. https://doi.org/10.1002/pen.24855
2. Saini T et al (2025) Polyvinyl alcohol: Recent advances and applications in sustainable materials. Polymer-Plastics Technol Mater 64(6):794–825. https://doi.org/10.1080/25740881.2024.2438046
3. Abdullah ZW et al (2017) PVA, PVA blends, and their nanocomposites for biodegradable packaging application. Polym-Plast Technol Eng 56(12):1307–1344. https://doi.org/10.1080/03602559.2016.1275684
4. Paradossi G et al (2003) Poly (vinyl alcohol) as versatile biomaterial for potential biomedical applications. J Mater Science: Mater Med 14(8):687–691. https://doi.org/10.1023/A:1024907615244
5. Shah N et al (2025) Tailored Polyvinyl Alcohol-Based Composites with Natural Additives for Biomedical and Soft Contact Lens Applications. Results Eng 107622. https://doi.org/10.1016/j.rineng.2025.107622
6. Khan MMR et al (2024) Synthesis, rheology, morphology, and mechanical properties of biodegradable PVA-based composite films: A review on recent progress. Processes 12(12):2880. https://doi.org/10.3390/pr12122880
7. Almarashi JQ, Abdel-Kader M (2020) Exploring nano-sulfide enhancements on the optical, structural and thermal properties of polymeric nanocomposites. J Inorg Organomet Polym Mater 30(8):3230–3240. https://doi.org/10.1007/s10904-020-01482-0
8. Ribeiro T, Baleizão C, Farinha JPS (2014) Functional films from silica/polymer nanoparticles. Materials 7(5):3881–3900. https://doi.org/10.3390/ma7053881
9. Lee DW, Yoo BR (2016) Advanced silica/polymer composites. J Ind Eng Chem 38:1–12. http://dx.doi.org/10.1016/j.jiec.2016.04.016
10. Bryaskova RG et al (2026) Advances in Polymer Micelles for Cancer Therapy: From Conventional to Smart Delivery Systems. Pharmaceutics 18(2):177. https://doi.org/10.3390/pharmaceutics18020177

11. Ensminger Y et al (2025) Polyglycerol-Based Lipids: A Next-Generation Alternative to PEG in Lipid Nanoparticles for Advanced Drug Delivery Systems. Macromolecular Rapid Communications e00428. https://doi.org/10.26434/chemrxiv-2025-2jf8r-v3
12. Kim A et al (2023) Recent progress in PEG-based composite phase change materials. Polym Rev 63(4):1078–1129. https://doi.org/10.1080/15583724.2023.2220041
13. Liu Z et al (2016) Preparation and properties of polyethylene glycol based semi-interpenetrating polymer network as novel form-stable phase change materials for thermal energy storage. Energy Build 127:327–336. http://dx.doi.org/10.1016/j.enbuild.2016.06.009
14. Qi GQ et al (2014) Polyethylene glycol based shape-stabilized phase change material for thermal energy storage with ultra-low content of graphene oxide. Sol Energy Mater Sol Cells 123:171–177. https://doi.org/10.1016/j.solmat.2014.01.024
15. Qi GQ et al (2015) Enhanced comprehensive performance of polyethylene glycol based phase change material with hybrid graphene nanomaterials for thermal energy storage. Carbon 88:196–205. http://dx.doi.org/10.1016/j.carbon.2015.03.009
16. Sawatari C, Kondo T (1999) Interchain hydrogen bonds in PVA/PEO blends. Macromolecules 32(6):1949–1955. https://api.semanticscholar.org/CorpusID:73672144
17. Mousa E et al (2021) Optical Study on PVA/PEG Blend Doped with Nano-Silica. J Electron Mater 50(5):2594–2604. https://doi.org/10.1007/s11664-021-08785-z
18. AlAbdulaal T et al (2025) Synthesis, structure, and optical properties of Fe2O3: PVA/PVP/PEG polymeric nanocomposite sheets for low-cost optical limiters under laser and solar visible lights. J Mater Sci: Mater Electron 36(28):1813. https://doi.org/10.1007/s10854-025-15871-z
19. Kadhim WK, Habeeb MA (2024) Ameliorating and tailoring the morphological, structural, and dielectric characteristics of SiO2/NiO futuristic nanocomposites doped PVA-PEG for nanoelectronic and energy storage applications. Silicon 16(16):5817–5832. https://doi.org/10.1007/s12633-024-03121-6
20. Dilshad MR et al (2021) Effect of silica nanoparticles on carbon dioxide separation performances of PVA/PEG cross-linked membranes. Chem Pap 75(7):3131–3153. https://doi.org/10.1007/s11696-020-01486-7
21. Zhang H et al (2023) Silicone-enhanced PVA hydrogels for high performance wearable strain sensors. Mater Design 229:111911. https://doi.org/10.1016/j.matdes.2023.111911
22. Ahmed H, Hashim A (2022) Exploring the characteristics of new structure based on silicon doped organic blend for photonics and electronics applications Silicon 14(9):4907–4914. https://doi.org/10.1007/s12633-021-01258-2
23. Obaid MN et al (2024) The effect of MgO nanoparticle on PVA/PEG-based membranes for potential application in wound healing. J Biomaterials Sci 35(13):1963–1977. https://doi.org/10.1080/09205063.2024.2364526
24. Al-Shehri S et al (2024) Synthesis of multifunctional flexible polymeric PVA/PEG blend nanocomposite films filled with AZO nanoparticles. Polym Bull 81(16):14561–14585.

https://doi.org/10.1007/s00289-024-05407-6

25. Mohammed B et al (2021) Improving the Optical Properties of PVA/PEG Blend Doped with BaTiO3 NPs. J Phys Conf Ser https//. 10.1088/1742-6596/1963/1/012005
26. Hayder N et al (2022) Analysis of Dielectric Properties of PVA/PEG/In2O3 Nanostructures for Electronics Devices. J Compos Adv Mater 32(5). https://doi.org/10.18280/rcma.320507
27. Abbas MH et al (2023) Enhanced dielectric characteristics of Cr2O3 nanoparticles doped PVA/PEG for electrical applications. Rev Compos Mater Av 33(4):261. https://doi.org/10.18280/rcma.330407
28. Heiba ZK et al (2022) Exploring the physical properties of PVA/PEG polymeric material upon doping with nano gadolinium oxide. Alexandria Eng J 61(5):3375–3383. https://doi.org/10.1016/j.aej.2021.08.051
29. Habeeb MA et al (2025) Synthesis and tuning the morphological, structural, optical and dielectric features of SiO2/CuO futuristic nanocomposites doped PVA–PEG for optoelectronic and energy storage applications. J Inorg Organomet Polym Mater 35(4):2391–2405. https://doi.org/10.1007/s10904-024-03334-7
30. Kadhim WK, Habeeb MA (2024) Synthesis and tailoring the morphological, structural and optical characteristics of SiO2–CO2O3 nanomaterials doped PVA–PEG for optoelectronic and food packing applications. Opt Quant Electron 56(8):1346. https://doi.org/10.1007/s11082-024-07275-w
31. Mohammed MK et al (2022) Effect of Titanium Nitrate Nanoparticles on Optical Properties of PVA/PEG Blend for Optoelectronics Detectors. Revue des Compos et des matériaux avancés 32(6):305. https://doi.org/10.18280/rcma.320606
32. Hashim A et al (2023) Improved Dielectric properties of PVA/PEG/TiN nanocomposites for ElectronicsApplications. Nanosistemi Nanomateriali Nanotehnologii 21(1):0125–0132. https://doi.org/10.15407/nnn.21.01.125
33. Tang CM et al (2015) Poly (vinyl alcohol) nanocomposites reinforced with bamboo charcoal nanoparticles: mineralization behavior and characterization. Materials 8(8):4895–4911. https://doi.org/10.3390/ma8084895
34. Hong X et al (2018) Dry-wet spinning of PVA fiber with high strength and high Young's modulus. IOP Conf Ser Mater Sci Eng. http://dx.doi.org/10.1088/1757-899X/439/4/042011
35. Siddaiah T et al (2018) Structural, optical and thermal characterizations of PVA/MAA: EA polyblend films. Mater Res 21(5):e20170987. https://doi.org/10.1590/1980-5373-MR-2017-0987
36. Ahmed HT, Abdullah OG (2019) Preparation and composition optimization of PEO: MC polymer blend films to enhance electrical conductivity. Polymers 11(5):853. https://doi.org/10.3390/polym11050853
37. Guan Y et al (2015) Physically crosslinked composite hydrogels of hemicelluloses with poly (vinyl alcohol phosphate) and chitin nanowhiskers. 10(1):1378–1393. https://doi.org/10.15376/biores.10.1.1378-1393
38. Tzitzios V et al (2006) Chemical synthesis and characterization of hcp Ni nanoparticles. Nanotechnology 17(15):3750–3755. http://dx.doi.org/10.1088/0957-4484/17/15/023

39. Papadopoulos L et al (2021) Comparative study of crystallization, semicrystalline morphology, and molecular mobility in nanocomposites based on polylactide and various inclusions at low filler loadings. Polymer 217:123457. https://doi.org/10.1016/j.polymer.2021.123457
40. Terzopoulou Z et al (2019) Interfacial interactions, crystallization and molecular mobility in nanocomposites of Poly (lactic acid) filled with new hybrid inclusions based on graphene oxide and silica nanoparticles. Polymer 166:1–12. https://doi.org/10.1016/j.polymer.2019.01.041
41. Vasques ALQ et al (2008) Size dependent photoluminescence of Si nano-crystals embedded in amorphous silicon. Solid State Phenomena 131:71–76. https://doi.org/10.4028/www.scientific.net/SSP.131-133.71
42. Abdelrazek EM et al (2018) Structural, optical, morphological and thermal properties of PEO/PVP blend containing different concentrations of biosynthesized Au nanoparticles. J Mater Res Technol 7(4):419–431. https://doi.org/10.1016/j.jmrt.2017.06.009
43. Fanta GM et al (2020) Phase behavior of amorphous/semicrystalline conjugated polymer blends. Polymers 12(8):1726. http://dx.doi.org/10.3390/polym12081726
44. Ramazanov M et al (2023) Structure and optic properties of the nanocomposites based on polypropylene and amorphous silica nanoparticles. J Thermoplast Compos Mater 36(4):1762–1774. http://doi.org/10.1177/08927057211028890
45. Altorbaq AS et al (2022) Crystallization kinetics and nanoparticle ordering in semicrystalline polymer nanocomposites. Prog Polym Sci 128:101527. https://doi.org/10.1016/j.progpolymsci.2022.101527
46. Wadkin-Snaith D et al (2023) Filler-induced heterogeneous nucleation of polymer crystals investigated by molecular dynamics simulations. Polymer 281:126113. https://doi.org/10.1016/j.polymer.2023.126113
47. Ming Y et al (2022) Polymer Nanocomposites: Role of modified filler content and interfacial interaction on crystallization. Eur Polymer J 162:110894. https://doi.org/10.1016/j.eurpolymj.2021.110894
48. Ning N et al (2012) Realizing the enhancement of interfacial interaction in semicrystalline polymer/filler composites via interfacial crystallization. Prog Polym Sci 37(10):1425–1455. https://doi.org/10.1016/j.progpolymsci.2011.12.005
49. Rana M et al (2021) Studies on optical signal due to oxygen effect on hydrogenated amorphous/crystalline silicon thin films. Appl Phys A 127(3):192. https://doi.org/10.1007/s00339-021-04322-1
50. Stern T (2025) Deciphering the triple-peak COC stretching FTIR absorbance consistently occurring in semicrystalline PEG. Polymers 17(16):2199. https://doi.org/10.3390/polym17162199
51. Hsiao KY et al (2025) Identification of Hydroxyl and polysiloxane compounds via infrared absorption spectroscopy with targeted noise analysis. Polymers 17(11):1533. https://doi.org/10.3390/polym17111533
52. Mansur HS et al (2008) FTIR spectroscopy characterization of poly (vinyl alcohol) hydrogel with different hydrolysis degree and chemically crosslinked with glutaraldehyde. Mater Sci Eng C

28(4):539–548. https://doi.org/10.1016/j.msec.2007.10.088

53. Nandiyanto A et al (2023) Interpretation of Fourier transform infrared spectra (FTIR): A practical approach in the polymer/plastic thermal decomposition. Indonesian J Sci Technol 8(1):113–126. https://doi.org/10.17509/ijost.v8i1.53297
54. Karthikeyan B et al (2019) Optical, vibrational and fluorescence recombination pathway properties of nano SiO2-PVA composite films. Opt Mater 90:139–144. https://doi.org/10.1016/j.optmat.2019.01.063
55. Panigrahi R et al (2020) Elucidating the role of interfacial hydrogen bonds on glass transition temperature change in a poly (Vinyl Alcohol)/SiO2 polymer-nanocomposite by noncovalent interaction characterization and atomistic molecular dynamics simulations. Macromol Rapid Commun 41(21):2000240. https://doi.org/10.1002/marc.202000240
56. Fahmy A et al (2020) Structure/property relationship of polyvinyl alcohol/dimethoxydimethylsilane composite membrane: Experimental and theoretical studies. Spectrochimica Acta A 228:117810. https://doi.org/10.1016/j.saa.2019.117810
57. Holland B, Hay J (2001) Thermal degradation of PVA. Polymer 42(16):6775–6783. https://doi.org/10.1016/S0032-3861(01)00166-5
58. Taghizadeh MT et al (2015) The investigation of thermal decomposition pathway and products of poly (vinyl alcohol) by TG-FTIR. J Appl Polym Sci 132(25). https://doi.org/10.1002/app.42117
59. Chiellini E et al (2003) Biodegradation of poly (vinyl alcohol) based materials. Prog Polym Sci 28(6):963–1014. https://doi.org/10.1016/S0079-6700(02)00149-1
60. Camino G et al (2001) Polydimethylsiloxane thermal degradation Part 1. Kinetic aspects. Polymer 42(6):2395–2402. https://doi.org/10.1016/S0032-3861(00)00652-2
61. Himawan A et al (2025) Formulation and evaluation of PVA-based composite hydrogels: physicochemical, leachables, and in vitro immunogenicity studies. J Mater Chem B 13(7):2431–2445. https://doi.org/10.1039/D4TB02181A
62. Park JS et al (2001) On the Viscoelastic Properties of Poly (vinyl alcohol) and Chemically Crosslinked Poly (vinyl alcohol). J Appl Polym Sci 82(7):1816–1823. https://doi.org/10.1002/app.2023
63. Mohammed M, El-Sayed F (2023) PEG's impact as a plasticizer on the PVA polymer's structural, thermal, mechanical, optical, and dielectric characteristics. Opt Quant Electron 55(13):1141. https://doi.org/10.1007/s11082-023-05420-5
64. Bershtein VA et al (2012) Dynamics, thermal behaviour and elastic properties of thin films of poly (vinyl alcohol) nanocomposites. RSC Adv 2(4):1424–1431. https://doi.org/10.1039/C1RA00535A
65. Al-Hussam AM et al (2016) Development of Thermal and Electrical Properties of Poly (vinyl alcohol)/Poly (ethylene glycol) Based on solid Electrolyte and Nanocomposite. Thamar Univ J 6(1):93–104. https://doi.org/10.59167/tujnas.v6i6.1331
66. Reguieg F et al (2020) Thermal characterization by DSC and TGA analyses of PVA hydrogels with organic and sodium MMT. Polym Bull 77(2):929–948. https://doi.org/10.1007/s00289-019-02782-3

67. Darabian B et al (2020) Improvement in mechanical properties and biodegradability of PLA using poly (ethylene glycol) and triacetin for antibacterial wound dressing applications. Prog Biomater 9(1):45–64. https://doi.org/10.1007/s40204-020-00131-6
68. Coşkun M et al (2025) MgO NPs reinforced PCL/PVC nanocomposite films with enhanced UV shielding and thermal stability for packaging applications. Open Phys 23(1):20250240. https://doi.org/10.1515/phys-2025-0240
69. Arthanareeswaran G et al (2008) Effect of silica particles on cellulose acetate blend ultrafiltration membranes: Part I. Sep Purif Technol 64(1):38–47. https://doi.org/10.1016/j.seppur.2008.08.010
70. Gudadur KS, Veluswamy P (2023) Flexible reversible polymer nano-composite thin film patch for wearable temperature sensor. Surf Interfaces 39:102975. https://doi.org/10.1016/j.surfin.2023.102975
71. Mirasadi K et al (2026) 4D printing of magnetically responsive shape memory polymers: toward sustainable solutions in soft robotics, wearables, and biomedical devices. Adv Sci 13(15):e13091. https://doi.org/10.1002/advs.202513091
72. Sringam J et al (2025) Shape memory performance and microstructural evolution in PLA/PEG blends: role of plasticizer content and molecular weight. Polymers 17(2):225. https://doi.org/10.3390/polym17020225
73. Staszczak M et al (2022) Characterization of polyurethane shape memory polymer and determination of shape fixity and shape recovery in subsequent thermomechanical cycles. Polymers 14(21):4775. https://doi.org/10.3390/polym14214775
74. Ju C et al (2026) Graphene Oxide-Modulated CMC/PVA Films with on-Demand Shape Recovery and Self-Healing Performance. Macromol Rapid Commun 47(4):2500345. https://doi.org/10.1002/marc.202500345
75. Falqi FH et al (2022) PVA/PEG/graphene shape memory composites responsive to multi-stimuli. Appl Phys A 128(5):427. https://doi.org/10.1007/s00339-022-05484-2

Figures

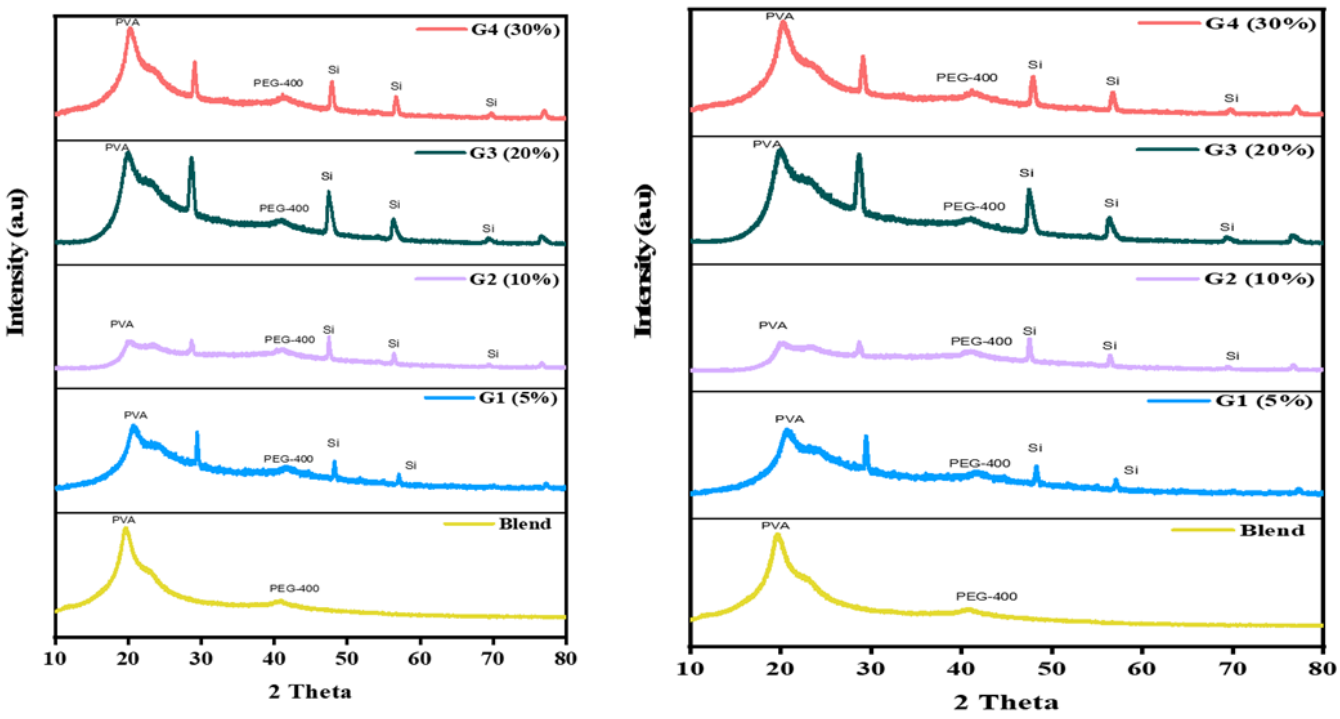


Figure 1

XRD patterns of PVA/PEG composites with varying silicon content (G1–G4).

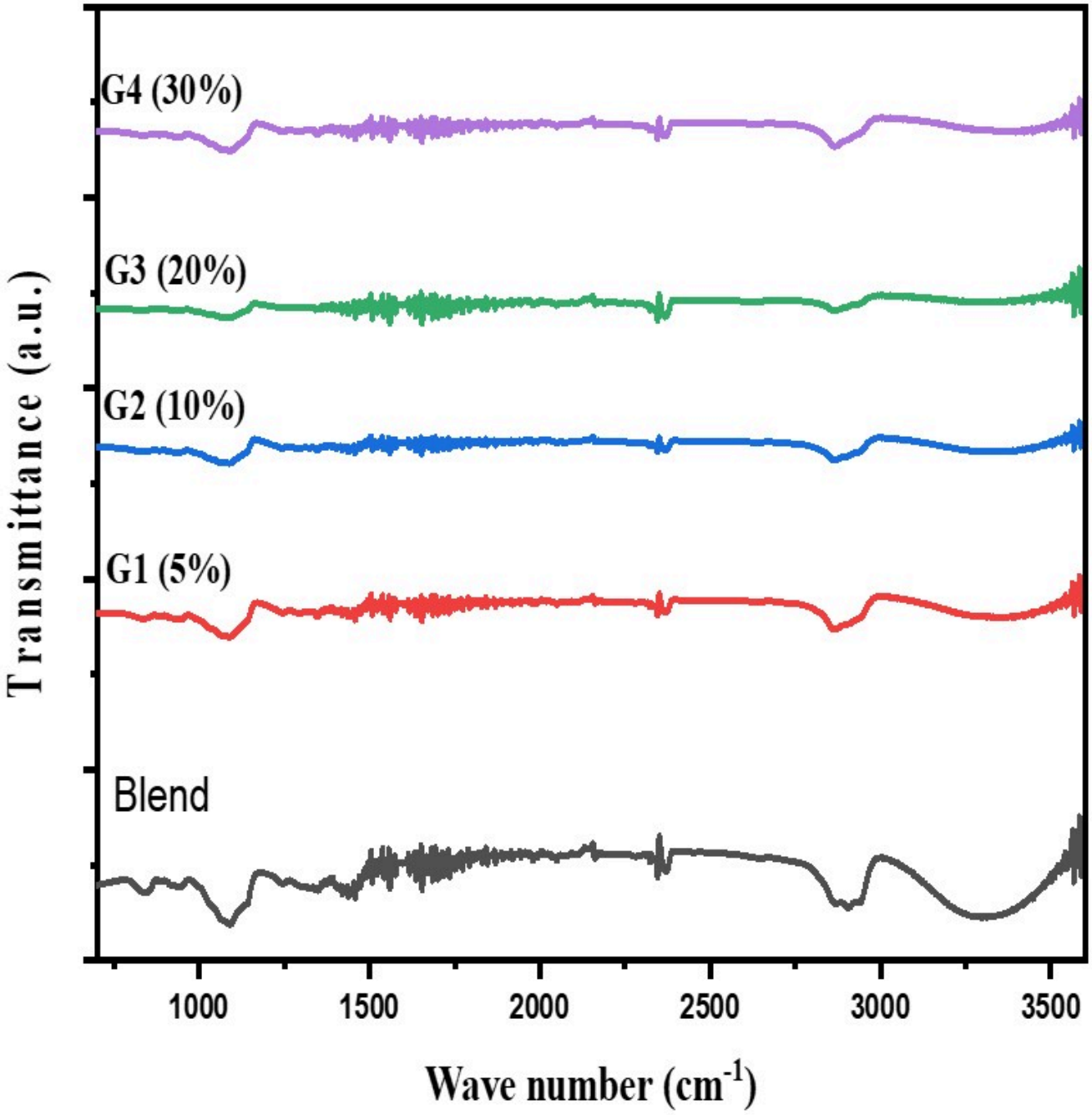


Figure 2

FTIR spectra of PVA/PEG and silicon-filled composites (G1–G4).

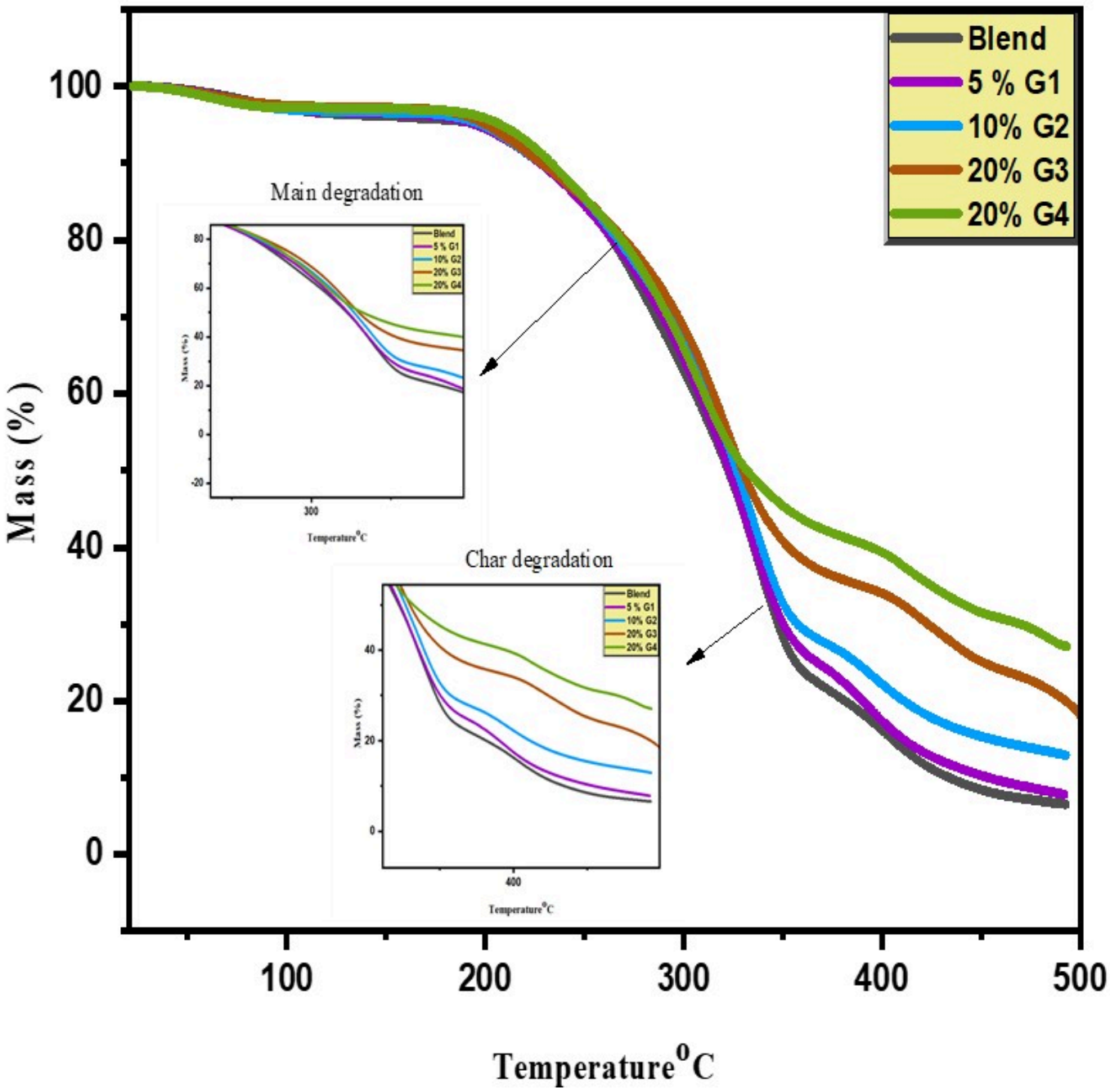


Figure 3

TGA curves of PVA/PEG and silicon-containing composites.

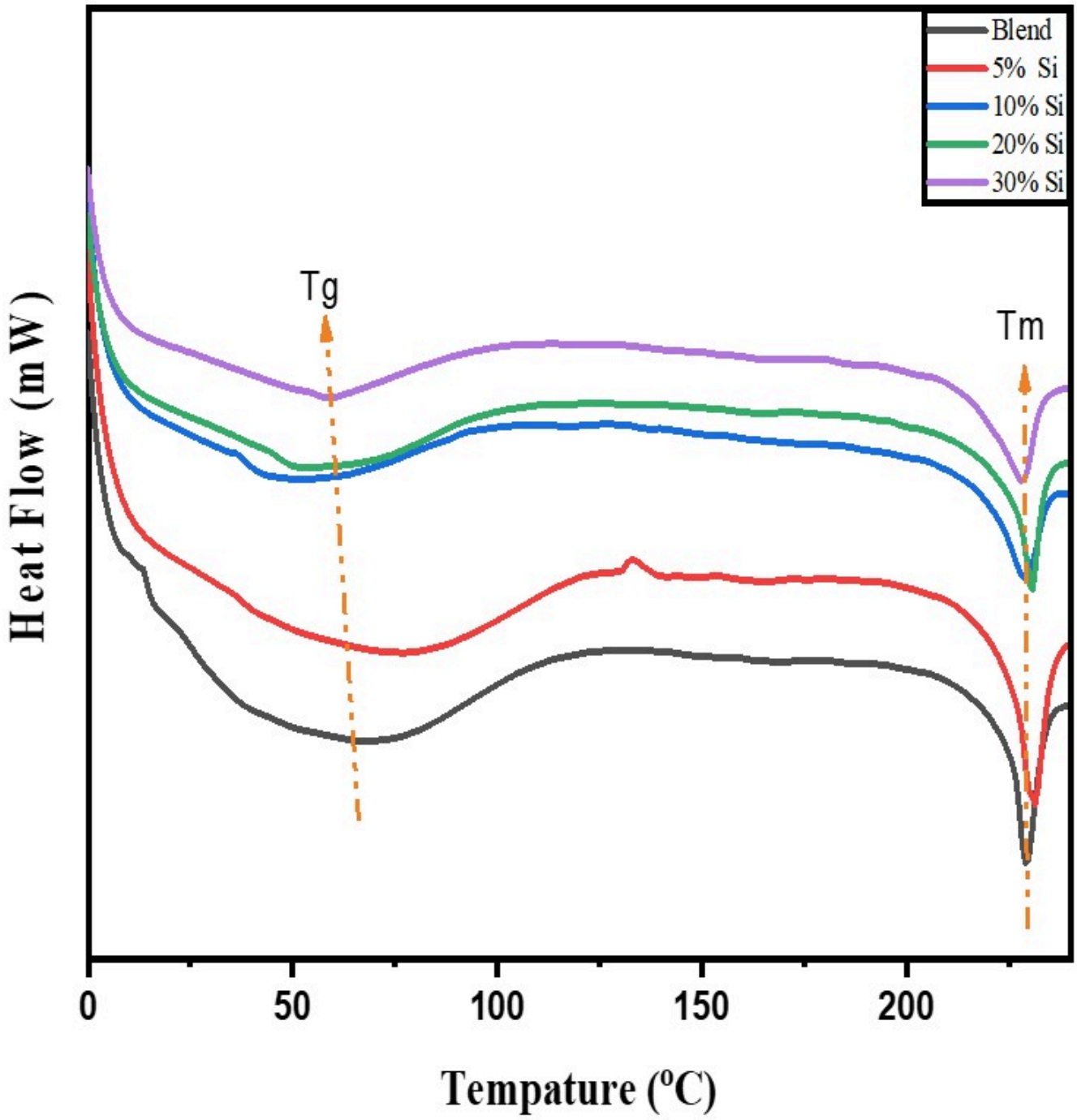


Figure 4

DSC curves of PVA/PEG and silicon-containing composites.

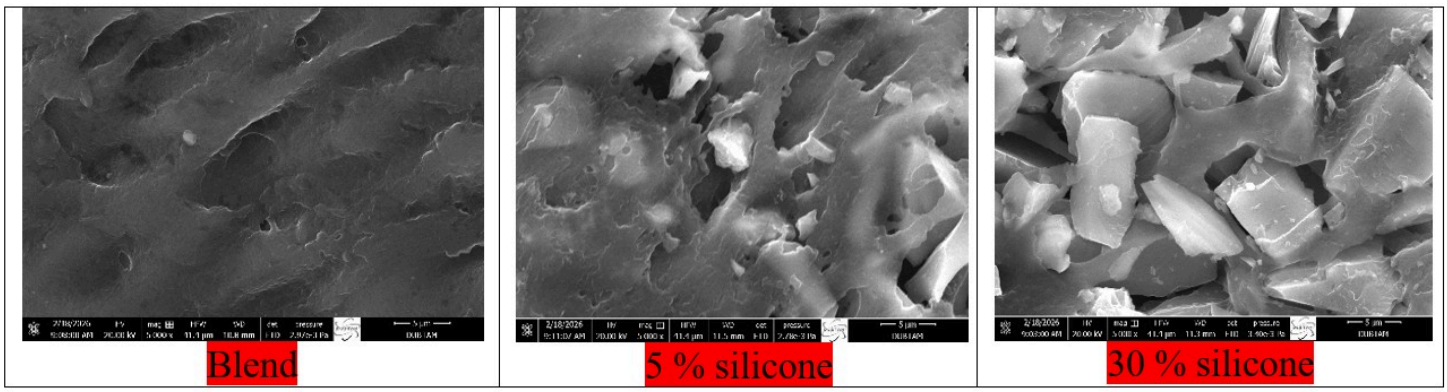


Figure 5

SEM image of blend and 5 %, 30 % silicone blend composites respectively.



Figure 6

Shape memory behavior of PVA/PEG/silicone composite: deformation, fixation, and recovery.

Supplementary Files

This is a list of supplementary files associated with this preprint. Click to download.

- floatimage1.png